A Kinetic Model for Cardiac PET with [1-Carbon-11]-Acetate

J. van den Hoff, W. Burchert, H.G. Wolpers, G.J. Meyer and H. Hundeshagen
Departments of Nuclear Medicine and Cardiology, Medical School Hannover, Germany

Carbon-11-labeled acetate is a unique tracer for noninvasive assessment of myocardial oxidative metabolism with PET. Because adequate kinetic models have been missing, data evaluation in the past was performed mostly with phenomenological approaches such as mono- or biexponential fitting which cannot account for the influence of finite input duration and blood volume encountered in noninvasive PET investigations. **Methods:** To investigate to what extent the current data evaluation schemes are justified, we developed a comprehensive model of [1-^{11}C]-acetate kinetics in the myocardium which incorporates five tissue compartments: free acetate, activated acetate, CO_2 precursors, amino acids and CO_2. We derived the analytical solution of the model equations which is used for simulations and data fitting. **Results:** The five-compartment model can reproduce in detail known experimental data. The resulting values of the eight model parameters compare favorably with existing biochemical facts. We have established the relation between parameters of the detailed model and one- and two-compartment models used for the evaluation of PET investigations. **Conclusion:** The kinetics of [1-^{11}C]-acetate are adequately described by a five-compartment model. One- and two-compartment models are sufficient for simultaneous quantitative assessment of myocardial oxidative metabolism and perfusion with [1-^{11}C]-acetate and PET.

Key Words: carbon-11-acetate; kinetic modeling; myocardial perfusion; oxidative metabolism; PET

J Nucl Med 1996; 37:521–529

The successful investigation of [1-^{11}C]-acetate as tracer for assessing myocardial oxidative metabolism (*1–6*) has initiated various clinical PET investigations (*8,9,13–21*). Acetate has therefore been suggested as marker of myocardial viability. Furthermore, the high extraction of acetate in the myocardium indicates the possibility of evaluating perfusion with this tracer (*7–9*).

Acetate is primarily metabolized in the tricarboxylic acid (TCA) cycle accompanied by the release of CO_2. Tissue clearance of the label after single capillary transit of an intracoronary bolus injection can be described by a biexponential decrease whose onset is delayed by a few minutes (*2,27*). The decay constant of the fast component of a biexponential fit, as well as the decay constant of a restricted monoexponential fit, correlate linearly with myocardial oxygen consumption (MVO_2) (*2,3*).

In PET investigations, monoexponential fitting has been almost exclusively (*1,4,6,9–11,13–21,23*). This procedure is inaccurate because it ignores temporal extension and variation of tracer delivery to tissue, as well as the contribution of blood activity to measured tissue activity due to finite fractional blood volume and spillover. The use of a simple one-compartment model improves the systematic accuracy of data evaluation because it accounts for these effects (*10*). Despite these improvements, such a model is still phenomenological; neither the physiological correlate of the tissue compartment nor the relation between model parameters and biochemical transport constants can be specified without a thorough analysis of acetate kinetics in the myocardium. Recently, Ng et al. (*27*) proposed a model for the description of acetate kinetics but excluded the very early phase of tissue clearance from data evaluation. Model simplifications important for data evaluation in PET were not investigated.

We present a less complex compartment model which can precisely reproduce the whole time course of measured tissue clearance curves, including the very early phase before onset of biexponential decrease. Simplifications of the model are investigated to allow parameter identification in PET.

MATERIALS AND METHODS

Theory

Metabolic Fate of [1-^{11}C]-Acetate in Myocardium. After extraction from blood, acetate is activated to acetyl-CoA. Acetyl-CoA then enters the TCA cycle by an essentially irreversible aldol condensation with oxaloacetate to citrate. Loss of the carbon label from the TCA cycle is mainly in the form of CO_2 (*2,3,22*). Apart from this major pathway, the most important reaction removing the label from the cycle is the reaction α-ketoglutarate $\rightarrow$ glutamate. Quantitatively less important reactions transfer the label to other amino acids (precursor: oxaloacetate).

Tracer kinetics strongly depend on location of the carbon label in the acetate molecule. The label from the C-1 position (i.e., in the carboxyl group) cannot be released as CO_2 in the first pass through the cycle but is lost completely in the second pass. In the case of [2-^{11}C]-acetate, loss of the label as CO_2 cannot occur during the first and second pass and probability of release is only 50% in each additional pass, which leads to much larger total leakage into the amino acid pools. Thus, [1-^{11}C]-acetate is more suitable for assessing oxidative metabolism. For this tracer, the TCA cycle constitutes a chain of reactions terminating in the second pass with the reaction α-ketoglutarate $\rightarrow$ succinyl-CoA + CO_2 (Fig. 1). For simplicity, 'TCAs I' incorporates TCA cycle intermediates prior to the first α-ketoglutarate formation and 'TCAs II' intermediates after α-ketoglutarate formation until isocitrate formation in the second pass.

Detailed Compartment Model for [1-^{11}C]-Acetate

Under resting conditions, the behavior of acetate in the myocardium can be summarized as follows:

- Initial washout (first 30 sec) is very fast (half-time below 5 sec) (*2*).
- Net extraction after single capillary transit: about two-thirds of injected dose (*2,4*).
- Acetate is activated to acetyl-CoA within a few seconds (*24,25*).
- Onset of rapid CO_2 release is delayed by about 2–3 min (*2*).

Received Jan. 5, 1995; revision accepted Aug. 22, 1995.
For correspondence or reprints contact: J. van den Hoff, PhD, Abteilung Nuklearmedizin und spezielle Biophysik, Zentrum Radiologie, Hannover, Konstanty-Gutschow-Strasse 8, 30625 Hannover, Germany.

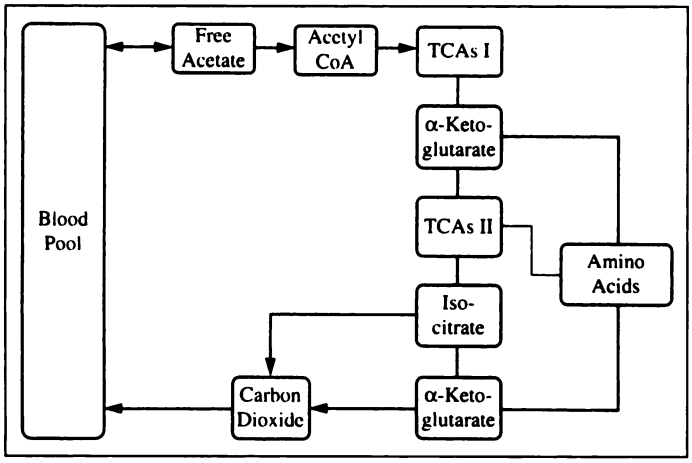

FIGURE 1. Metabolic pathway of [1-^{11}C]-acetate in myocardium. Principal transport steps of the ^{11}C label are shown. 'TCAs I' and 'TCAs II' incorporate tricarboxylic acid (TCA) cycle intermediates through which the label passes.

- Labeling of all TCA cycle intermediates takes several minutes (*24,25*).
- After the initial delay, CO_2 release is biexponential (*2*).
- Maximum clearance rate: about 10% per minute in the rapid phase (*2,4*).

Based on these statements and the chain of transport steps described above, we propose a five-compartment model (Fig. 2) to describe [1-^{11}C]-acetate kinetics: Compartment 1 (free acetate) accounts for initial rapid exchange of tracer with blood pool. Limited net extraction of acetate is interpreted as being due to competition between free backdiffusion and activation. The time constant of the initial washout phase is $(k_2 + k_3)^{-1}$ and single-capillary transit net extraction equals $k_3/(k_2 + k_3)$. Compartment 2 (activated acetate) accounts for acetyl-CoA and part of the TCA cycle intermediates. This compartment causes delayed onset of rapid tissue clearance. Compartment 3 (CO_2 precursors) represents the remaining TCA cycle intermediates. According to data from Ng et al. (*27*), mitochondrial and cellular glutamate might also be included. Compartments 3 and 4 determine the tissue response at later times. Compartment 4 (amino acids) accounts mainly for glutamate and its derivatives and explains the second exponential in the tissue response. Compartment 5 (CO_2) accounts for the fact that the CO_2 washout rate is limited.

The coupled linear differential equations describing the model and the analytical solution of these equations are given in the Appendix. This solution enables rapid simulations of tissue response curves under various conditions and fitting of experimental data.

Armbrecht et al. (*2*) measured tissue clearance curves after single capillary transit of an intracoronary bolus injection with good time resolution (1 sec) and statistical accuracy. The analytical solution was fitted to these data with a nonlinear least squares minimization algorithm, which yields simultaneously parameter estimates and their covariance matrix.

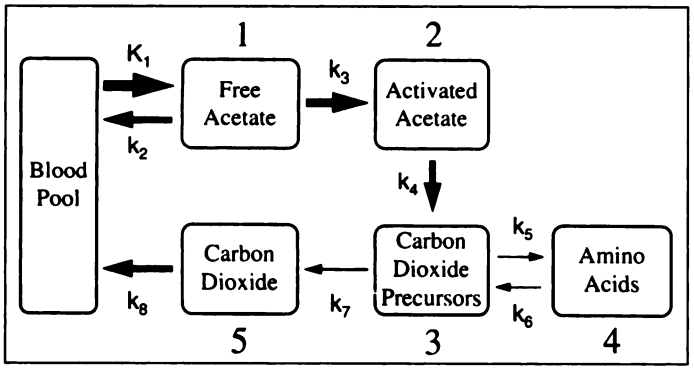

FIGURE 2. Detailed compartment model of [1-^{11}C]-acetate kinetics in myocardium. Arrow thickness indicates magnitude of rate constants.

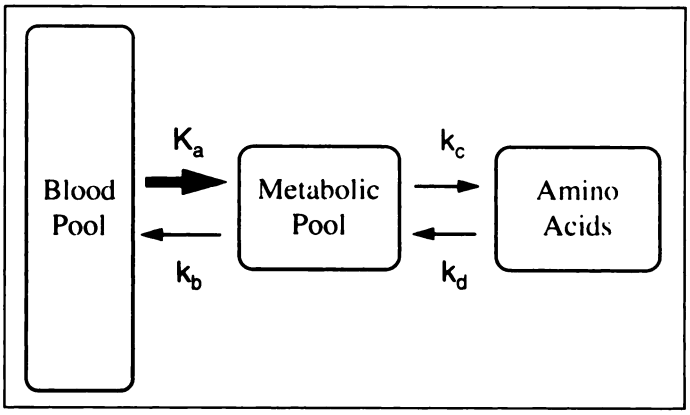

FIGURE 3. Simplified compartment model of [1-^{11}C]-acetate kinetics in myocardium. Arrow thickness indicates magnitude of rate constants.

Model Reduction

To describe all features of the system's impulse response, the complete model presented above is necessary. On the other hand, it is not feasible to identify all model parameters in PET investigations because of insufficient temporal sampling, limited statistical accuracy and finite input duration. Therefore, a model reduction is needed which still enables assessment of perfusion and metabolism.

Neglecting the small CO_2 fraction, tissue clearance is completely determined by compartments 3 and 4 when steady state is reached in previous compartments because compartments 1 and 2 only translate the arterial input into a modified input of compartment 3 (Eq. A2). Justified by the asymptotic behavior of the system response at later times, we propose an effective two-compartment model (Fig. 3) to evaluate PET investigations: if data evaluation could be restricted to late times, the parameters k_b, k_c and k_d of the restricted model would be identical to k_7, k_5 and k_6, respectively (neglecting the CO_2 contribution). In practice, the time range for data fitting cannot be restricted sufficiently without losing too much statistical accuracy. Moreover, it would not be possible to obtain a stable estimate of perfusion. It is therefore necessary to include the early portion of the time-activity curve in the evaluation and to determine the relation between the parameters of the simplified and detailed model.

Computer Simulations

To investigate the effects of model simplifications, we computed tissue response curves for the detailed model with various parameter sets. These response curves were then fitted using the simplified model. The relation between the parameters of simplified and detailed model is thus obtained directly. The effect of reducing the simplified model to a one-compartment model was also investigated.

Data Acquisition

The PET scans were performed with an ECAT 951/31 PET scanner (Siemens/CTI, Erlangen, Germany). The resolution of the reconstructed image data (31 slices (plane separation: 3.4 mm), 128 × 128 matrices (pixel size: 2.3 × 2.3 mm), Hann filter with cutoff 0.3) was about 9–10 mm FWHM. The data were corrected for attenuation (20-min transmission) and radioactive decay. The procedure described by Meyer et al. (*28*) was used to synthesize [1-^{11}C]-acetate.

Simultaneously with bolus injection of 1.1 GBq [1-^{11}C]-acetate, dynamic scanning (10 × 10 sec, 1 × 60 sec, 5 × 100 sec, 3 × 180 sec, 4 × 300 sec) was started. The arterial input function was

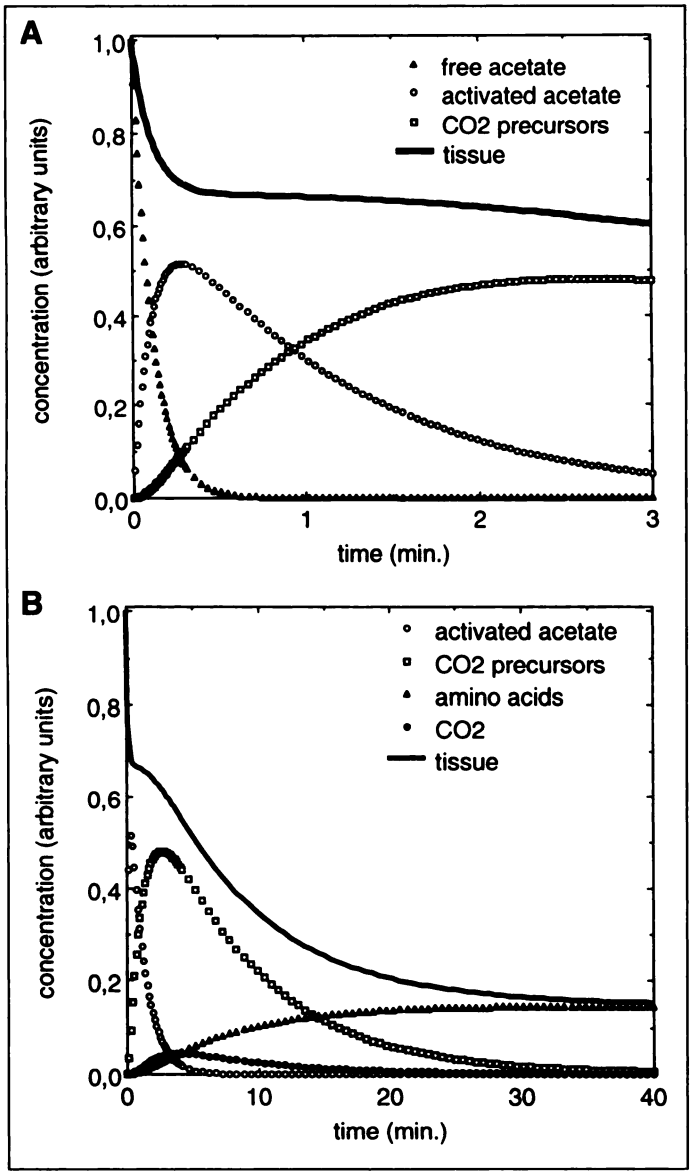

FIGURE 4. Impulse response of the detailed compartment model (Fig. 2). The analytical solution of the model equations (Appendix A) was used for the calculations. (A) The first 3 min after impulse input. Contributions of amino acids and CO_2 are small in this time range and are not shown. (B) The first 40 min after impulse input. Contribution of free acetate is small in this time range and is not shown.

determined in the reconstructed images from a region in the cavum of the left ventricle.

Patients and Study Protocol

The study group consisted of 41 patients (aged 60 ± 10 yr) more than 2 wk after acute Q-wave infarction. ECG infarct locations were anterior in 21 patients, posterior in 13 and both in 7 patients. Routine coronary angiography was performed in all patients. Left ventricular ejection fraction was 42% ± 15%. Myocardial blood flow and oxidative metabolism were assessed by dynamic [1-^{11}C]-acetate PET. The local ethics committee reviewed and approved the PET and angiographic protocols, and informed consent was obtained from each patient.

RESULTS

Comparison of Model Prediction and Measured Impulse Response

Figure 4 shows an example of a calculated unit impulse response. The rate constants (Table 1) are derived from a least

TABLE 1
Values of Model Parameters Used in Figure 4*

Parameter	Value	Physiological correlate
K_1	1	blood flow (free diffusion assumed)
k_2	3	backflow of unmetabolized acetate
k_3	6	conversion to acetyl-CoA
k_4	0.9	transfer into TCA cycle
k_5	0.03	transfer into amino acid pool
k_6	0.003	backflow from amino acid pool
k_7	0.1	oxidative metabolism
k_8	1	CO_2 washout

*K_1 in units of ml/min/ml, k_2–k_8 in units of min^{-1}.

squares fit of the model to the data of Armbrecht et al. [Figs. 1A and 1B of (*2*)]. Results are given in Figure 5. Deviations between data and fit are small (Fig. 5B) and show no systematic trend above 0.5%. The quoted accuracies of the parameter

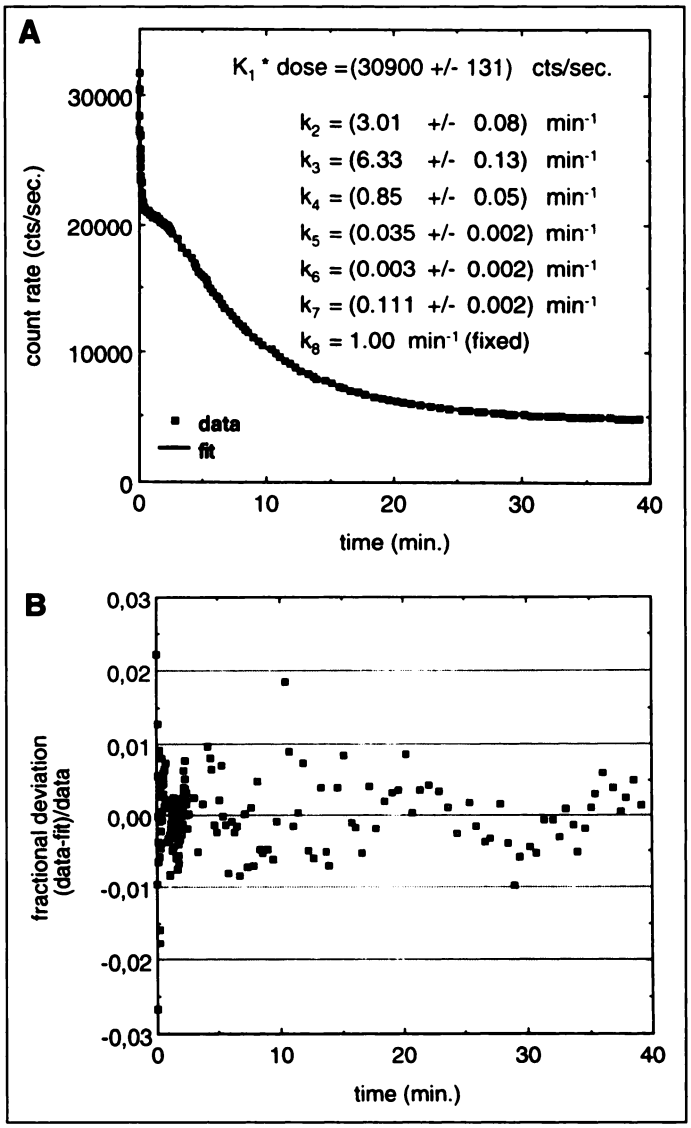

FIGURE 5. Least squares fit of the model (Fig. 2) to the data of Armbrecht and coworkers (*2*). (A) Experimental data (squares) and fit (solid line). Deviations between data and fit are not resolved on this scale. Fitted values (mean ± s.d.) are shown in the plot. (B) Fractional deviations between data and fit. Deviations do not show any systematic trend above a threshold of 0.5%.

estimates in Figure 5A are derived from the covariance matrix of the model parameters.

In our model, tracer exchange between blood pool and tissue is treated as free diffusion so that K_1 equals flow, F. Therefore, K_1 = 1 ml/min/ml is used in Table 1, which is the average flow consistent with a net extraction of about 65% [Figs. 1B and 3 of (*2*)]. According to the model, net extraction is given by

$$E(F) = \frac{k_3}{k_2(F) + k_3} = \frac{1}{1 + \frac{k_2(F)}{k_3}} = \frac{1}{1 + \frac{F}{ptc \cdot k_3}}, \quad \text{Eq. 1}$$

where ptc = K_1/k_2 is the free acetate distribution volume. By using the values of Table 1, ptc = 1/3. Equation 1 agrees with the data of Armbrecht et al. [Fig. 3 of (*2*)] up to a flow of about 3 ml/min/ml. Deviations occur only at high flow levels. In this regime, Equation 1 predicts a monotonic decrease of E(F).

Parameter Identification: Statistical Accuracy and Ambiguous Solutions

Statistical accuracy is described by the covariance matrix of the fit. In our fits, only k_4 and k_8 exhibited a large covariance and low statistical accuracy. Other covariances were small, indicating weak parameter interaction. The different parameters influence the system's impulse response as follows:

- K_1 determines the scaling (amplitude) of the impulse response. Due to rapid washout of free acetate, determination of K_1 (i.e., initial uptake) is only possible if data from the initial washout phase are included.
- k_2 and k_3 are determined precisely by the initial washout and plateau phase: the initial washout rate is $k_2 + k_3$, and the single capillary transit net extraction is $k_3/(k_2 + k_3)$.
- k_4 and k_8 show a strong interaction because both parameters influence the shape of the response during the plateau phase. This is the reason for the observed large covariance. We have fixed k_8 to a value of 1 min^{-1} which is in accord with the good diffusibility of CO_2 (and also with the inaccurately fitted value of 0.93 min^{-1}), k_4 then becomes a stable parameter.
- k_5, k_6 and k_7 are responsible for biexponential tissue clearance. The small size of k_6 precludes its accurate determination within the given time window up to 40 min.

Different sets of parameters can result in exactly the same system response curves by modifying the contributions from different compartments without altering the sum. We derived the following results from an inspection of the model equations (Appendix).

The total tissue response is not effected by exchange of k_4 and k_8, that is, a second solution exists with $k_4(2) = k_8(1)$ and $k_8(2) = k_4(1)$. This ambiguity is removed by fixing k_8 to a physiologically reasonable value which is necessary to obtain a statistically reliable estimate of k_4.

In the limit of vanishing k_6: the total tissue response is not effected by the transformation

$$k_4(2) = k_5(1) + k_7(1),$$

$$k_5(2) = \frac{k_4(1)}{k_5(1) + k_7(1)} \cdot k_5(1),$$

$$k_7(2) = \frac{k_4(1)}{k_5(1) + k_7(1)} \cdot k_7(1). \quad \text{Eq. 2}$$

When Equation 2 and Table 1 are used, the alternative parameters are $k_4(2)$ = 0.13 min^{-1}, $k_5(2)$ = 0.21 min^{-1} and $k_7(2)$ = 0.69 min^{-1}. Selection of a specific parameter set has to be based on additional information.

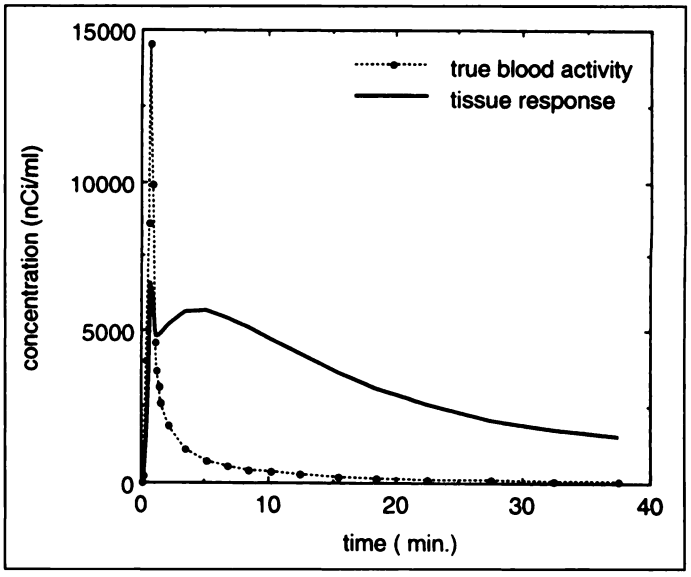

FIGURE 6. Calculated tissue response (solid line) of the detailed model (Fig. 2) after a typical bolus injection (dotted line). An effective blood volume contribution of 30% is taken into account.

Influence of Model Reduction on Parameter Estimates

The analytical solution of the detailed model—including a fractional blood volume term—was used to generate response curves from a typical experimental input function. The simulated curves were then fitted with the simplified model.

In these simulations, K_1 and k_7 were varied over the physiological range of values. Free diffusion of acetate between blood and tissue implies a fixed ratio K_1/k_2, which is the distribution volume for free acetate. Therefore, $k_2 = 3K_1$ (Table 1) was used in the simulations. The other parameters were fixed according to Table 1, with the exception of k_5. Since we are primarily interested in human studies, k_5 was reduced to 0.01 min^{-1} to comply with the experimental tissue response; in human studies the fraction of the label transferred to the amino acid pool is obviously smaller than in the canine studies of Armbrecht et al. (*2*). Figure 6 shows the input function (corrected for metabolites) plus simulated response for K_1 = 1 ml/min/ml, k_7 = 0.1 min^{-1} and an effective blood volume (fbv plus spillover) of 30%.

Within the usual measurement interval of 40 min, the data are compatible with a vanishing k_6. Therefore, we used $k_d = 0$ when fitting the simplified model. In addition, we fitted the data up to 20 min with the one-compartment model that resulted by setting $k_c = 0$. Several limiting cases were investigated.

K_1 Proportional to k_7. This is to be expected if blood flow essentially controls the rate of oxidative metabolism. A ratio K_1/k_7 = 10 (Table 1) was used in this case. Results are shown in Figure 7.

k_7 Constant, K_1 Variable. This corresponds to a decoupling of flow and metabolism (as given during pharmacological vasodilation or possibly in hypoperfused tissue). Results are shown in Figure 8.

K_1 Constant, k_7 Variable. This also corresponds to a decoupling of flow and metabolism. Results are shown in Figure 9.

Apart from the K_a obtained directly from the fit, the figures also show the affect of extraction correction ($K_a^{cor} = K_a/E$) according to Armbrecht et al. (*2*) or the correction expected from Equation 1.

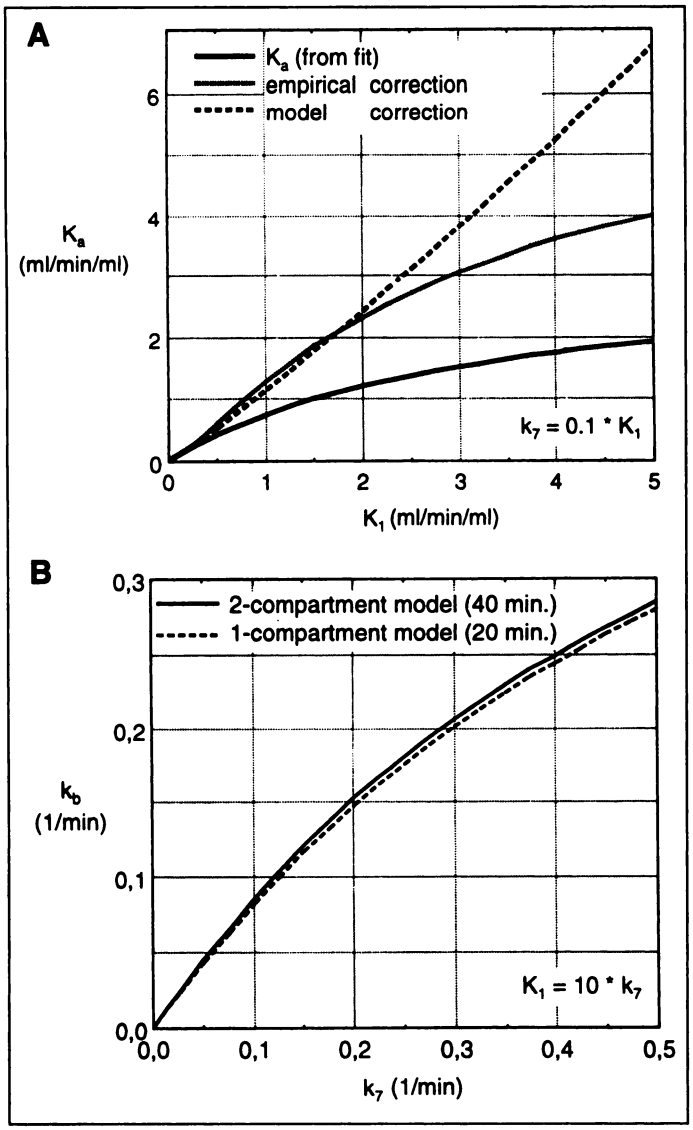

FIGURE 7. Relation between parameters of detailed model (Fig. 2) and simplified model (Fig. 3). Dependence on K_1 and k_7 for a fixed ratio K_1/k_7 = 10. (A) Dependence of K_a on K_1. Proportionality is maintained for normal and reduced flows if an extraction correction is performed. K_a is not altered by data evaluation of the first 20 min with a one-compartment model. (B) Dependence of k_b on k_7. Approximate proportionality is maintained over a wide range of values. Data evaluation of the first 20 min with a one-compartment model (dashed line) yields similar results.

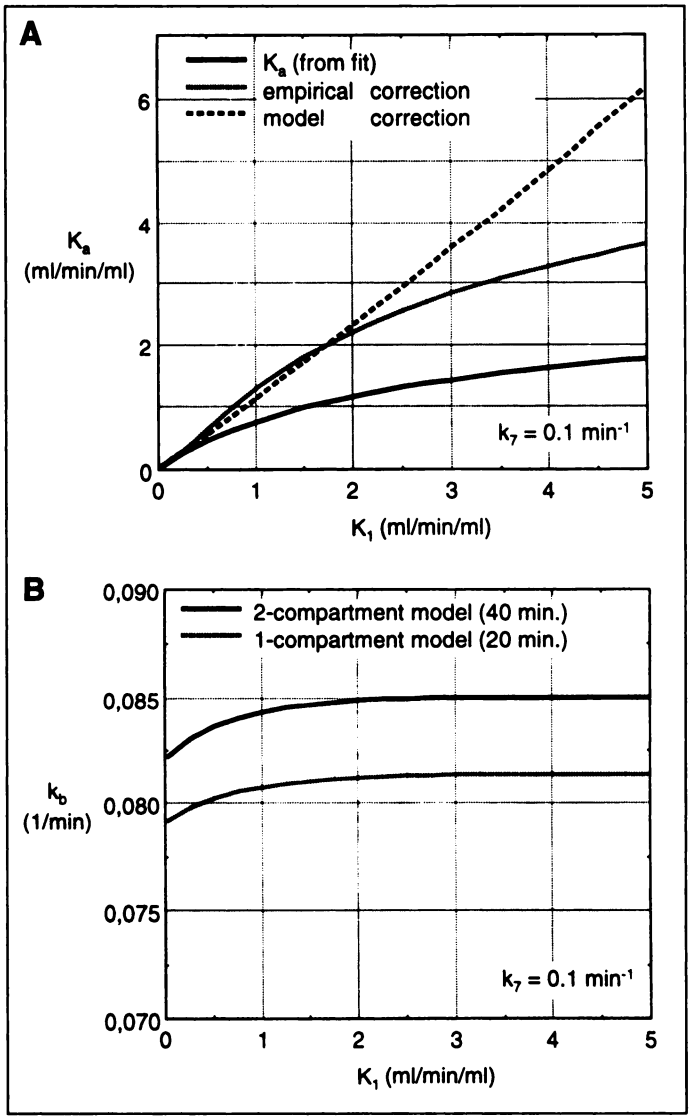

FIGURE 8. Relation between parameters of detailed model (Fig. 2) and simplified model (Fig. 3). Dependence on K_1 for a constant value of k_7 = 0.1 min^{-1}. (A) Dependence of K_a on K_1. Proportionality is maintained for normal and reduced flows if an extraction correction is performed. K_a is not altered by data evaluation of the first 20 min a with one-compartment model. (B) Essentially no dependence of k_b on K_1. Data evaluation of the first 20 min with a one-compartment model (dashed line) yields similar results.

Patient Studies

The one- and two-compartment models were used for data evaluation. An example of tissue response in infarcted and remote myocardium and the corresponding fit of the two-compartment model is given in Figure 10. In accord with the simulations the one compartment model is sufficient for correct determination of K_a and k_b if data evaluation is restricted to the first 20 min after injection. Fractional blood volume was included as a free parameter in the fitting procedure. An average metabolite correction of the input function according to the data of Buck (*10*) was performed. Extraction correction according to Armbrecht (*2*) was applied to the fitted K_a values in order to derive absolute flow values. Results are given in Table 2.

DISCUSSION

Model Validity

Our model accurately reproduces all details of the experimental impulse response such as rapid initial washout of unmetabolized acetate; single capillary transit net extraction; delayed onset of biexponential clearance (plateau phase); and rates and amplitudes of both exponentials in biexponential clearance phase.

The statistical accuracy of the parameter estimates as derived from the covariance matrix is high (except for k_4, if k_8 is not fixed). Model simplifications lead to a failure of reproducing all features of the curve simultaneously. Both findings indicate that our model represents the least complex configuration necessary for the description of acetate kinetics in the myocardium. Recently, Ng et al. (*27*) proposed a model which tries to approximate the pathway of Figure 1 more closely by introducing two separate CO_2 precursor pools and corresponding amino acid pools. We think this to be an unjustified increase in model complexity as long as parameter identification is based solely on total tissue response curves, because the increased number of parameters cannot be determined with sufficient statistical accuracy. In this model, tissue clearance after initial delay is explained by significant contributions from five compartments which do not seem to be identifiable in the response curve, (cf. (*27*), Table 1, Figs. 7 and 8). Fitting the normoxic response

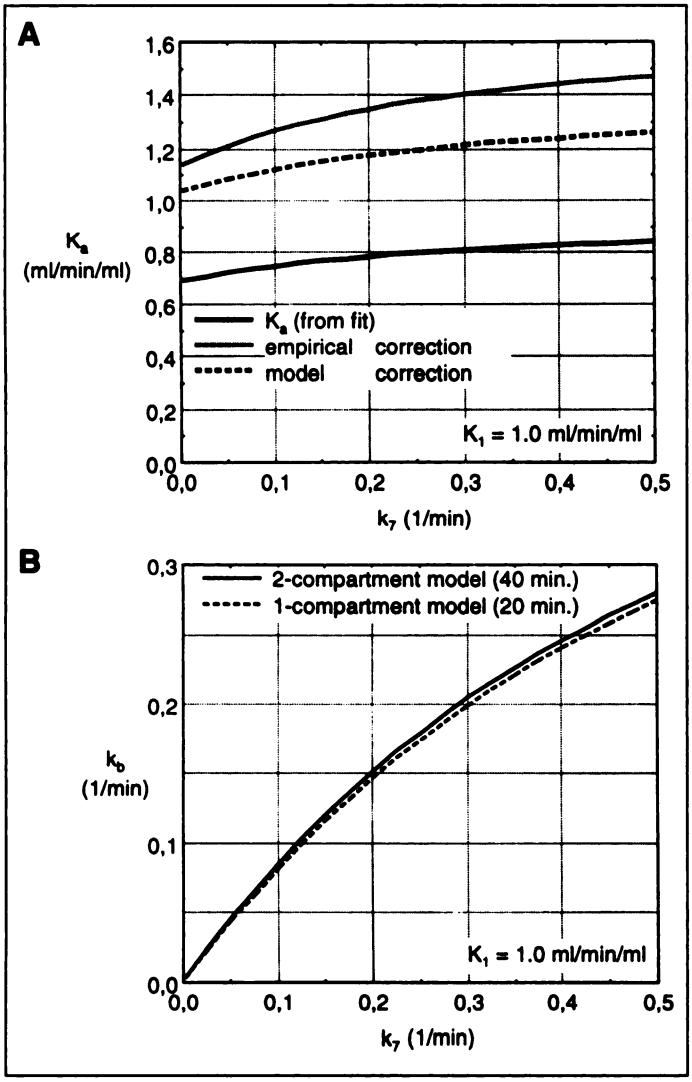

FIGURE 9. Relation between parameters of detailed model (Fig. 2) and simplified model (Fig. 3). Dependence on k_7 for a constant value of K_1 = 1 ml/min/ml. (A) Essentially no dependence of K_a on k_7. K_a is not altered by data evaluation of the first 20 min with a one-compartment model. (B) Dependence of k_b on k_7. Approximate proportionality is maintained over a wide range of values. Data evaluation of the first 20 min with a one-compartment model (dashed line) yields similar results.

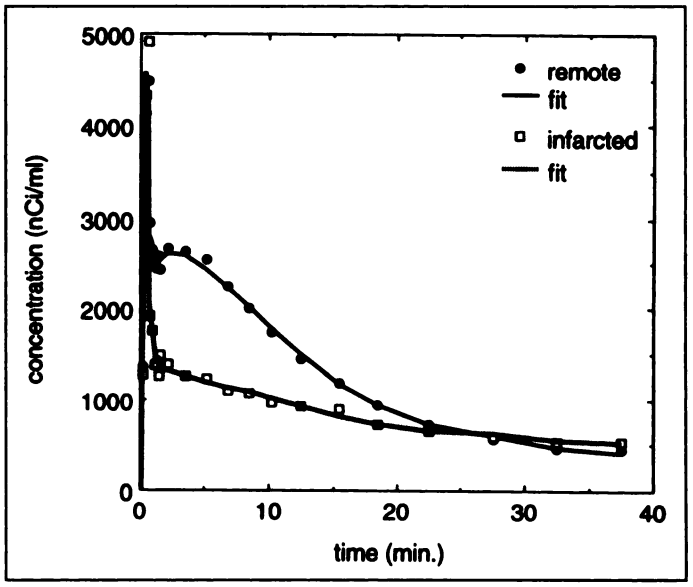

FIGURE 10. Tissue response in infarcted and remote myocardium. The PET data together with fits of the two-compartment model are shown. Flow is 1.3 and 0.3 ml/min/ml in remote and infarcted myocardium, respectively. Clearance rate k_b is 0.15 and 0.07 min^{-1}, respectively. Fractional blood volume (plus spillover) is 41% and 51%, respectively.

curve (calculated from Table 1 in Ng et al.) with our model gives perfect agreement despite reduction to only three compartments contributing to the response after initial delay. We think that the use of a single compartment (no. 3 in Fig. 2) for most of the TCA cycle intermediates is sufficient because the experimental data show that essentially two pools control the shape of the tissue response at later times. This indicates that production of CO_2 is a bottleneck reaction and that steady state can be maintained between the different intermediates of the cycle during the whole clearance phase. The values of the rate constants derived from the fit (Table 1) can further be checked against independent information.

k_2 = 3 min^{-1} is the rate of free acetate washout. Because conversion of acetate to acetyl-CoA mainly takes place inside the mitochondria, the distribution volume of readily diffusible acetate is expected to be exterior to the mitochondria. It has been estimated that about half of the cytoplasmic volume of cardiac cells consists of mitochondria (*26*). One would thus expect a distribution volume below 50%. Our model predicts a value of about one-third, presuming the data of Armbrecht [Fig. 1 of (*2*)] correspond to a flow of 1 ml/min/ml. From Figure 3 of (*2*), it is obvious that this need not be the case. If the data correspond to a somewhat higher flow, the value of the distribution volume is increased accordingly. In any case, the model yields a reasonable order of magnitude for the distribution volume.

k_3 = 6 min^{-1} is the rate of conversion from acetate to acetyl-CoA and compares favorably with the fact that this reaction is known to take place within a few seconds (*24,25*).

k_4 = 0.9 min^{-1} is the transfer rate into the CO_2 precursor pool and determines the duration of the plateau phase before onset of rapid tissue clearance. The value is consistent with the finding that labeling of all TCA intermediates takes several minutes (*24,25*). Due to the ambiguity in determining the parameters k_4, k_5 and k_7, the question has to be addressed as to which of the two possible solutions is physiologically reasonable. Accepting the second solution ($k_4(2)$ = 0.13 min^{-1}, $k_5(2)$ = 0.21 min^{-1}, $k_7(2)$ = 0.69 min^{-1}) results in sizeable tracer concentrations only in compartments 2 and 4 a few minutes after bolus passage. Transfer into the CO_2 precursor pool would be the rate-limiting step and the experimentally observed correlation between tissue clearance and MVO_2 would mainly be caused by regulation of the initial condensation of acetyl-CoA with oxaloacetate. Furthermore, one would expect a slow

TABLE 2
Results from Rest Investigations in 41 Patients with Myocardial Infarction (>2 Weeks) in Remote and Infarcted Myocardium*

Parameter	Mean ± s.d.	Minimum	Maximum
$K_a^{(remote)}$	0.69 ± 0.13	0.44	1.03
$K_a^{(infarction)}$	0.26 ± 0.13	0.02	0.58
$k_b^{(remote)}$	0.12 ± 0.03	0.07	0.21
$k_b^{(infarction)}$	0.08 ± 0.03	0.01	0.15
$Flow^{(remote)}$	1.15 ± 0.29	0.62	1.92
$Flow^{(infarction)}$	0.32 ± 0.20	0.02	0.89
Age (yr)	59.7 ± 10.1	38	78
CK_{max}	953 ± 724	54	2735
RPP	9735 ± 1572	6240	12090

*K_a and flow are in units of ml/min/ml; k_b in units of min^{-1}; CK_{max} in U/liter.

(due to the small k_4), but nearly synchronous (due to the fast intra-TCA cycle rates) labeling of all intermediates, which contradicts the experimental finding. Finally, reactions of the TCA cycle incorporated in compartment 2 are also part of compartment 3, which additionally accounts for the CO_2 producing steps. Thus, it would be expected that k_7 is smaller than k_4. We have therefore adopted the solution corresponding to Table 1 as being more reasonable. To settle the question finally, it would be necessary to perform experiments that directly assess the contributions of the different compartments to the system response.

The initial rapid decrease of measured activity has been interpreted by Armbrecht et al. (*2*) as washout of nonextracted tracer. We think it is more likely that this phase reflects clearance of freely diffusible acetate from tissue because the plateau following the initial decrease is reached only after 15–20 sec [(*2*), Fig. 1B]. On the other hand, a capillary transit time of 1–2 sec and additional 1–2 sec for entering and leaving the field of view can be estimated, resulting in about 5 sec for complete passage. Neither duration nor exponential shape of the initial washout seems explainable as clearance of a spatially collimated bolus from the vascular bed. Free diffusion across the capillary wall further implies a constant distribution volume K_1/k_2, which leads to Equation 1. The concordance of Equation 1 with the data of Armbrecht et al. (*2*) supports our interpretation, at least for flow values that are not too high. The deviations at higher flow levels might indicate that the concepts of free diffusion and fixed distribution volume of acetate are no longer valid at high flow levels. On the other hand, the validity of the high flow data of Armbrecht et al. (*2*) might be questioned: a constant extraction fraction at high flow levels (after an initial decrease) implies that the net uptake rate does not saturate but increases proportional to flow in the high flow regime which is difficult to explain. A possible reason for erroneous results would be the failure to detect the complete bolus in the field of view because of larger spatial extension at high flow velocities.

In contrast to our approach, Ng et al. (*27*) excluded the early washout phase from data fitting because of the interpretation as washout of nonextracted tracer. Fitting of k_{01} and k_{21} (corresponding to k_2 and k_3 in our model) thus leads to inconsistencies. If the parameters are numerically large—which is to be expected—the first compartment is cleared before start of the fitting interval so that parameter identification becomes impossible. Parameter adjustment to small values might simply reflect this loss of identifiability. This could explain the otherwise surprising drop of k_{01} to 2% of its normoxic value in ischemia (and the synchronous drop in the largely unregulated activation to acetyl CoA). Furthermore, the definition of net extraction [Equation 7 of (*27*)] is questionable. If the first compartment is already cleared prior to onset of the plateau phase, net extraction simply is equal to first-pass extraction.

Model Simplification

The computer simulations demonstrated the possibility of simplifying the model drastically for quantitative assessment of flow and metabolism with PET.

A strong correlation between true blood flow (K_1) and the uptake parameter (K_a) of the simplified models is observed. Application of the model derived extraction correction according to Equation 1 yields a linear relationship between corrected K_a and K_1, which differs by about 20% from the line of identity. The difference arises because model reduction is not completely equivalent to replacement of flow K_1 by the net uptake $K_1 * k_3/(k_2 + k_3)$. Use of the average extraction correction published by Armbrecht et al. (*2*) yields essentially identical results below a flow of 2 ml/min/ml. Taking into account the rather large uncertainties of the corresponding data (cf. (*2*), Fig. 3) this empirical correction is compatible with the model prediction up to a flow of about 3 ml/min/ml. In this flow range, either correction allows to derive absolute flow values with a predicted overestimation of true flow by about 20%. The precise magnitude of the overestimate depends on the values chosen for the different model parameters in the simulations. We used the values given in Table 1 (except $k_5 = 0.01\ min^{-1}$), which are based on the data of Armbrecht et al. (*2*). If the principal features of the tissue response are not significantly modified, a good proportionality between the interesting parameters of the detailed and reduced model is always maintained.

The relation between k_b and the rate of CO_2 production, k_7, is also nearly linear with k_b being reduced by about 20% in comparison to k_7. This shows that k_b is well suited for assessing the rate of oxygen consumption. Therefore, we propose the reduced two-compartment model (including an extraction correction) for evaluation of the complete time course of PET investigations. Under resting conditions, additional reduction to a one-compartment model and data evaluation in a restricted time range up to 20 min postinjection yields essentially identical results.

Our model also establishes a relationship between true rate constants and decay constants determined in exponential fitting of the impulse response. Ambrecht et al. reported (*2*) that the rate constant of the fast biexponential component as well as the rate constant of a restricted monoexponential fit are proportional to the rate of oxidative metabolism. When adopting our model, this statement was not quite correct. By neglecting the small CO_2 contribution, the decay constant λ_f of the fast biexponential component is equal to the eigenvalue λ_4 (Appendix) but not equal to any of the system's rate constants. Now, $\lambda_4 \approx k_5 + k_7$ (because $k_6 \approx 0$) and a linear relation between λ_4 and k_7 is only obtained if k_5 is much smaller than k_7 (or if k_5 varies in proportion to k_7). The monoexponential rate constant λ_m is approximately proportional to k_7 for moderately small k_5/k_7 ratios if the time range of the fit is adequately restricted. This corresponds to the relation between k_b and k_7 for finite input duration using a one-compartment model. Obviously, the usefulness of λ_f and λ_m as a measure of oxidative metabolism depends on the relative size of k_5, k_6 and k_7, whereas interpreting the data in terms of the detailed model enables direct determination of k_7, i.e., the rate of the interesting metabolic step.

Patient Studies

The results presented in Figure 10 and Table 2 demonstrate that quantitative blood flow values can be derived under resting conditions with the simplified models. Further work must show if this is possible under stress conditions as well. Clearance rates are consistently higher than those derived from monoexponential fitting. This is in accord with previous results (*10,23*) and reflects the fact that finite input duration, recirculation and fractional blood volume are not considered in exponential fitting. The use of an average metabolite correction does not interfere with blood flow determination because of the rather slow increase of the metabolite fraction (*10,12*). Determination of the tissue clearance rate is affected only slightly because individual deviations from the average correction do not modify the true input function significantly, especially during the first few minutes of tracer delivery to tissue.

CONCLUSION

The model presented in this paper adequately describes the behavior of [1-^{11}C]-acetate in the myocardium and is consistent with current knowledge of its different reactions. The model yields the correct shape of the tissue response as well as physiologically reasonable values for the model parameters. It enables a better understanding of the different factors influencing the time-activity curve and provides explanations for experimental findings such as flow-dependence of net extraction and correlation between tissue clearance rate and MVO_2. The simplified model allows quantitative assessment of myocardial blood flow and oxidative metabolism in noninvasive PET investigations. As far as evaluation of metabolism is concerned, this finding is in accord with phenomenological approaches used in the past. The ability to simultaneously evaluate myocardial blood flow and metabolism allows assessment of myocardial viability with a single PET investigation.

APPENDIX

The model of Figure 2 is described by the following system of differential equations:

$$\frac{d\vec{c}}{dt}(t) = \hat{K}\vec{c}(t) + \vec{b}(t) \qquad \text{Eq. A1}$$

$$\text{with } \hat{K} = \begin{bmatrix} -(k_2+k_3) & 0 & 0 & 0 & 0 \\ k_3 & -k_4 & 0 & 0 & 0 \\ 0 & k_4 & -(k_5+k_7) & k_6 & 0 \\ 0 & 0 & k_5 & -k_6 & 0 \\ 0 & 0 & k_7 & 0 & -k_8 \end{bmatrix},$$

$$\vec{c}(t) = \begin{bmatrix} c_1(t) \\ c_2(t) \\ c_3(t) \\ c_4(t) \\ c_5(t) \end{bmatrix} \text{ and } \vec{b}(t) = \begin{bmatrix} K_1 c_a(t) \\ 0 \\ 0 \\ 0 \\ 0 \end{bmatrix}.$$

$\hat{K}$ is the rate matrix defining the structure of the model, $\vec{c}(t)$ is the vector of tracer concentrations in the different compartments. As usual, these concentrations are averages over whole tissue space and total tracer concentration is given by the sum of individual concentrations. $\vec{b}(t)$ is the vector of inputs from blood ($c_a(t)$: arterial tracer concentration).

The analytical solution is most easily obtained by noting that transport between tissue compartments is unidirectional with the exception of transport between compartments 3 and 4. The solution can therefore be found successively for different parts of the system. $c_1(t)$, $c_2(t)$, $c_5(t)$ are given by convolution of the impulse responses of the respective compartments with the input from their direct precursors. $c_3(t)$ and $c_4(t)$ are obtained by convolution of $c_2(t)$ with the impulse response of the subsystem 'compartment 3 plus compartment 4' which is structurally identical to the well known FDG model (including dephosphorylation). The final result is ($\otimes$ denotes convolution):

$$c_1(t) = c_a(t) \otimes K_1 e^{\lambda_1 t}, \qquad \text{Eq. A2}$$

$$c_2(t) = c_1(t) \otimes k_3 e^{\lambda_2 t},$$

$$c_3(t) = c_2(t) \otimes \frac{k_4}{\lambda_3 - \lambda_4}\left[(k_6 + \lambda_3)e^{\lambda_3 t} - (k_6 + \lambda_4)e^{\lambda_4 t}\right],$$

$$c_4(t) = c_2(t) \otimes \frac{k_4 k_5}{\lambda_3 - \lambda_4}\left[e^{\lambda_3 t} - e^{\lambda_4 t}\right],$$

$$c_5(t) = c_3(t) \otimes k_7 e^{\lambda_5 t},$$

where the decay constants are given by

$$\lambda_1 = -(k_2 + k_3), \qquad \text{Eq. A3}$$

$$\lambda_2 = -k_4,$$

$$\lambda_{3/4} = -\frac{k_5 + k_6 + k_7}{2} \pm \sqrt{\left(\frac{k_5 + k_6 + k_7}{2}\right)^2 - k_6 k_7},$$

$$\lambda_5 = -k_8.$$

For applications it is not advantageous to use Equation A2 directly because convolution with $c_a(t)$ usually has to be performed numerically. The subsequent numerical convolutions would introduce unnecessary errors in the calculations. It is therefore more accurate to first derive the unit impulse response by analytically calculating the successive convolutions of exponentials in Equation A2 and to perform the numerical convolution with $c_a(t)$ afterwards.

ACKNOWLEDGMENTS

The authors thank Professor Wolfgang Müller-Schauenburg, Dr. Oliver Seelberg and Dr. Herwig Weisser for valuable discussions and suggestions.

REFERENCES

1. Armbrecht JJ, Buxton DB, Brunken RC, Phelps ME, Schelbert HR. Regional myocardial oxygen consumption determined noninvasively in humans with [1-^{11}C]acetate and dynamic positron tomography. *Circulation* 1989;80:863–872.
2. Armbrecht JJ, Buxton DB, Schelbert HR. Validation of [1-^{11}C]acetate as a tracer for noninvasive assessment of oxidative metabolism with positron emission tomography in normal, ischemic, postischemic and hyperemic canine myocardium. *Circulation* 1990;81:1594–1605.
3. Brown M, Marshall DR, Sobel BE, Bergmann SR. Delineation of myocardial oxygen utilization with carbon-11-labeled acetate. *Circulation* 1987;76:687–696.
4. Brown MA, Myears DW, Bergmann SR. Noninvasive assessment of canine myocardial oxidative metabolism with carbon-11-acetate and positron emission tomography. *J Am Coll Cardiol* 1988;12:1054–1063.
5. Brown MA, Myears DW, Bergmann SR. Validity of estimates of myocardial oxidative metabolism with carbon-11-acetate and positron emission tomography despite altered patterns of substrate utilization. *J Nucl Med* 1989;30:187–193.
6. Buxton DB, Nienaber CA, Luxen A, et al. Noninvasive quantitation of regional myocardial oxygen consumption in vivo with [1-^{11}C]acetate and dynamic positron emission tomography. *Circulation* 1989;79:134–142.
7. Chan SY, Brunken RC, Phelps ME, Schelbert HR. Use of the metabolic tracer carbon-11-acetate for evaluation of regional myocardial perfusion. *J Nucl Med* 1991;32:665–672.
8. Gropler RJ, Siegel BA, Geltman EM. Myocardial uptake of carbon-11-acetate as an indirect estimate of regional myocardial blood flow. *J Nucl Med* 1991;32:245–251.
9. Krivokapich J, Huang SC, Schelbert HR. Assessment of the effects of dobutamine on myocardial blood flow and oxidative metabolism in normal human subjects using nitrogen-13-ammonia and carbon-11-acetate. *Am J Cardiol* 1993;71:1351–1356.
10. Buck A, Wolpers HG, Hutchins GD, et al. Effect of carbon-11-acetate recirculation on estimates of myocardial oxygen consumption by PET. *J Nucl Med* 1991;32:1950–1957.
11. Choi Y, Huang SC, Hawkins RA, et al. A refined method for quantification of myocardial oxygen consumption rate using mean transit time with carbon-11-acetate and dynamic PET. *J Nucl Med* 1993;34:2038–2043.
12. Shields AF, Graham MM, Kozawa SM, et al. Contribution of labeled carbon dioxide to PET imaging of carbon-11-labeled compounds. *J Nucl Med* 1992;33:581–584.
13. Beanlands RS, Bach DS, Raylman R, et al. Acute effects of dobutamine on myocardial oxygen consumption and cardiac efficiency measured using carbon-11-acetate kinetics in patients with dilated cardiomyopathy. *J Am Coll Cardiol* 1993;22:1389–1398.
14. Czernin J, Porenta G, Brunken R, et al. Regional blood flow, oxidative metabolism and glucose utilization in patients with recent myocardial infarction. *Circulation* 1993;88:884–895.
15. Gropler RJ, Geltman EM, Sampathkumaran K, et al. Comparison of carbon-11-acetate with fluorine-18-fluorodeoxyglucose for delineating viable myocardium by positron emission tomography. *J Am Coll Cardiol* 1993;22:1587–1597.
16. Hicks RJ, Savas V, Currie PJ, et al. Assessment of myocardial oxidative metabolism in aortic valve disease using positron emission tomography with ^{11}C acetate. *Am Heart J* 1992;123:653–664.
17. Kalff V, Hicks RJ, Hutchins G, Topol E, Schwaiger M. Use of carbon-11-acetate and dynamic positron emission tomography to assess regional myocardial oxygen consumption in patients with acute myocardial infarction receiving thrombolysis or coronary angioplasty. *Am J Cardiol* 1993;71:529–535.
18. Kotzerke J, Hicks RJ, Wolfe E, et al. Three-dimensional assessment of myocardial oxidative metabolism: a new approach for regional determination of PET-derived carbon-11-acetate kinetics. *J Nucl Med* 1990;31:1876–1883.
19. Tamaki N, Magata Y, Takahashi N, et al. Myocardial oxidative metabolism in normal subjects in fasting, glucose loading and dobutamine infusion states. *Ann Nucl Med* 1992;6:221–228.

20. Walsh MN, Geltman EM, Brown MA, et al. Noninvasive estimation of regional myocardial oxygen consumption by positron emission tomography with carbon-11-acetate in patients with myocardial infarction. *J Nucl Med* 1989;30:1798–1808.
21. Weinheimer CJ, Brown MA, Nohara R, Perez JE, Bergmann SR. Functional recovery after reperfusion is predicated on recovery of myocardial oxidative metabolism. *Am Heart J* 1993;125:939–949.
22. Wolfe RR, Jahoor F. Recovery of labeled CO_2 during the infusion of C-1- versus C-2-labeled acetate: implications for tracer studies of substrate oxidation. *Am J Clin Nutr* 1990;51:248–252.
23. Raylman RR, Hutchins GD, Beanlands SB, Schwaiger M. Modeling of carbon-11-ccetate kinetics by simultaneously fitting data from multiple ROIs coupled by common parameters. *J Nucl Med* 1994;35:1286–1291.
24. Randle PJ, England PJ, Denton RM. Control of the tricarboxylate cycle and its interaction with glycolysis during acetate utilization in rat hearts. *Biochem J* 1970; 117:677–695.
25. Chance EM, Seeholzer SH, Kobayashi K, Williamson JR. Mathematical analysis of isotope labeling in the citric acid cycle with applications to ^{13}C NMR studies in perfused rat hearts *J Biol Chem* 1983;258:13785–13794.
26. Olson MS. In: Devlin TM, ed. *Textbook of biochemistry*, 3rd ed. New York: Wiley-Liss Inc.; 1992:262.
27. Ng CK, Huang SC, Schelbert HR, Buxton DB. Validation of a model for [1-^{11}C]acetate as a tracer of cardiac oxidative metabolism. *Am J Physiol* 1994;266:H1304–H1315.
28. Meyer GJ, Guenther U, Matzke KH, Harms T, Hundeshagen H. A modified preparation method for [^{11}C]acetate preventing liquid phase extraction steps. *J Lab Compd Radiopharm* 1993;32:182–183.

(continued from page 5A)

FIRST IMPRESSIONS:
Multiple Bony Exostoses on Bone Scan

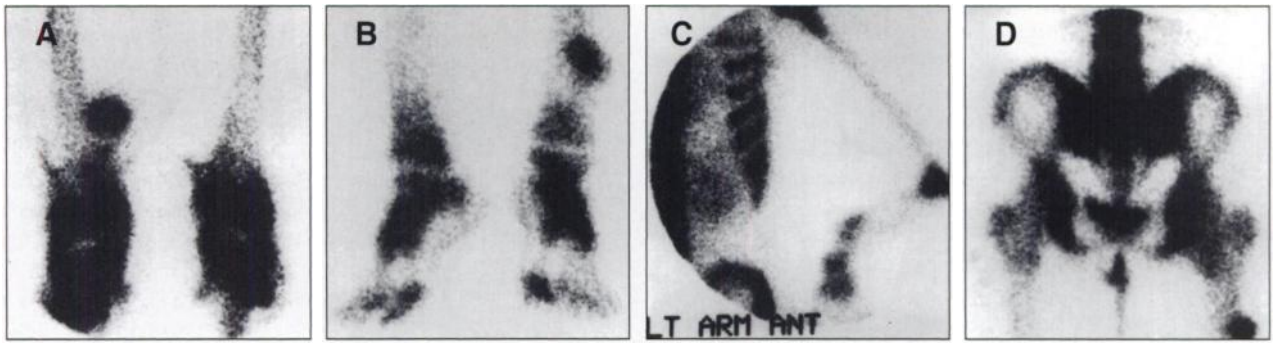

Figure 1.

Figure 2.

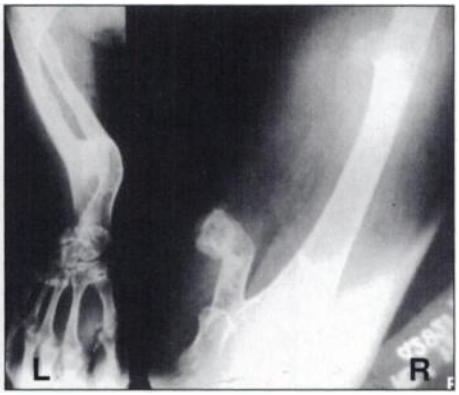

Figure 3.

PURPOSE
A 30-yr-old woman presented with swelling over the lower end of the right thigh, lower end of the left leg and deformity and swelling over the lower end of the left forearm. Bone scintigraphy revealed increased tracer uptake in all these regions as well as in the upper third of the right femur shaft (Fig. 1). A skeletal survey demonstrated bony exostosis in these regions (Figs. 2, 3)

TRACER
Technetium-99m-MDP, 740 MBq

ROUTE OF ADMINISTRATION
Intravenous

TIME AFTER INJECTION
4 hours

INSTRUMENTATION
Elscint SP-4 SPECT gamma camera with LEAP collimation

CONTRIBUTORS
S. Shikare, K. Bashir, G.H. Tilve, Seth G.S. Medical College and K.E.M. Hospital, Parel, Bombay, India